In situ manipulation of magnetic anisotropy in magnetite thin films

A. Brandlmaier,* S. Geprägs, M. Weiler, A. Boger, and M. Opel
Walther-Meissner-Institut, Bayerische Akademie der Wissenschaften, 85748 Garching, Germany

H. Huebl, C. Bihler, and M. S. Brandt
Walter Schottky Institut, Technische Universität München, 85748 Garching, Germany

B. Botters and D. Grundler
Physik-Department E10, Technische Universität München, 85748 Garching, Germany

R. Gross and S. T. B. Goennenwein†
Walther-Meissner-Institut, Bayerische Akademie der Wissenschaften and Physik-Department E23, Technische Universität München, 85748 Garching, Germany

(Received 3 December 2007; revised manuscript received 17 January 2008; published 31 March 2008)

We show that the ferromagnetic anisotropy of a thin crystalline Fe_3O_4 film can be manipulated *in situ* via the application of tunable stress. The stress is exerted by a piezoelectric actuator, onto which the Fe_3O_4 film is cemented. The strain in the sample is quantified as a function of the voltage applied to the actuator using high-resolution x-ray diffraction, and the corresponding evolution of the magnetic anisotropy is determined by ferromagnetic resonance spectroscopy. By this means, we are able to directly correlate structural and magnetic properties. The experimental results demonstrate that a piezoelectric actuator allows to substantially modify the magnetic anisotropy of a crystalline ferromagnetic thin film, enabling a voltage control of magnetization orientation. The possibility to orient the main elongation axis of the actuator along any given direction in the film plane opens a pathway for the investigation of the magnetoelastic properties of ferromagnetic thin films under tunable stress, shear, or combinations of both stress and shear.

DOI: 10.1103/PhysRevB.77.104445 PACS number(s): 75.30.Gw, 75.80.+q, 76.50.+g

I. INTRODUCTION

The presence of a spontaneous magnetization **M** is a key property of ferromagnets, which is exploited in magnetoelectronics and spintronics applications. For example, the orientation of the magnetization vector **M** is essential for the functionality of many magnetoelectric devices.[1,2] Usually, magnetic fields are used to control the magnetization orientation. However, this approach reaches its limits in modern, highly integrated magnetic microstructures, as cross-talk effects make it impossible to address individual magnetic bits. Thus, novel magnetization orientation control schemes are investigated vigorously. One such scheme relies on electronic correlation phenomena in multiferroics, e.g., the interaction between voltage-controllable ferroelectric polarization and ferromagnetism in these materials.[3–10] Another approach to alter the magnetization orientation without the need to apply magnetic fields relies on spin-torque effects.[11–13] Furthermore, a direct electric-field control of the magnetization orientation via electric fields has also been suggested.[14,15] Last but not least, the interaction between strain and magnetic properties, i.e., the magnetoelastic or the magnetostrictive effect, opens an avenue for strain control of the magnetization orientation. In particular, the correlation between strain, ferroelectricity, and ferromagnetism in multiferroics has been recently exploited by Eerenstein *et al.*[7] and Thiele *et al.*[10] to manipulate the magnetization via electric fields in epitaxial ferromagnetic thin film/ferroelectric substrate heterostructures.

In this paper, we show that the magnetic anisotropy of ferromagnetic thin films can be tuned continuously and reversibly *in situ* by means of strain in ferromagnetic thin film/piezoelectric actuator heterostructures. We use magnetite (Fe_3O_4) as a prototype ferromagnet, as this material unites a ferromagnetic Curie temperature $T_C \approx 860$ K (Ref. 16) well above room temperature with a high electron spin polarization $|P| \geq 55\%$.[17] Magnetite, therefore, is a promising material for spin injection devices. To introduce an *in situ* tunable strain into the magnetite thin film, we cement a piezoelectric actuator onto the Fe_3O_4 sample.[18,19] The expansion (or contraction) of the piezoelectric actuator as a function of the applied electric voltage V_{piezo} is directly transferred into the magnetite film, yielding a voltage-controllable strain contribution. To optimize the induced strain, we cement the magnetite film onto the piezoactuator face to face. In contrast to earlier studies,[19] we use x-ray diffraction, which allows us to directly measure the strain in the supporting MgO substrate and thus to quantify the variation in lattice constants. The changes of magnetic anisotropy induced by this piezostrain make it possible to shift the magnetization orientation by about 6° within the Fe_3O_4 film plane. A quantitative analysis of the experimental data shows that upon optimizing the strain transmission efficiency and the strain orientation, much larger magnetization orientation shifts will be possible. As the magnetostriction constant $\lambda_{100}^{Fe_3O_4} = -19.5 \times 10^{-6}$ (Ref. 20) of bulk Fe_3O_4 is comparable to those of, e.g., Fe, Ni, or CrO_2,[21,22] our results suggest that a piezostrain control of the magnetization orientation is a realistic and versatile scheme applicable to a variety of ferromagnets. Furthermore, the possibility to orient the main elongation axis of the piezoactuator along any direction within the ferromagnetic film plane during the cementing process allows us to intentionally

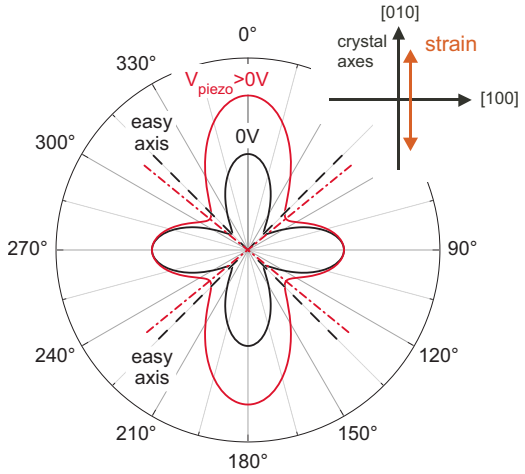

FIG. 1. (Color online) Angular dependence of the free energy on the orientation of magnetization. The application of lateral stress to a thin crystalline ferromagnetic film alters its magnetic anisotropy. Assuming that the ferromagnetic film is cubic and exhibits the characteristic in-plane fourfold symmetry of the cubic magnetic anisotropy contribution to free energy (black) for vanishing piezostrain, the application of stress along [010] with $K_{magel}/K_{c1}=-1/5$ (red) will result in tetragonal symmetry. For $\epsilon_2>0$ and $B_1>0$, the strain axis becomes magnetically harder, and the magnetic easy axes indicated by dashed lines are rotated towards [100].

select the type of strain (pure strain, shear strain, or combinations of both) exerted in the sample. Thus, a particular magnetoelastic response of the magnetic film can be selectively investigated or adjusted.

II. THEORETICAL BACKGROUND

A crystalline solid responds to an externally applied, uniaxial stress by a deformation. This deformation is described by the 3×3 strain tensor ϵ_{ij}, with $i,j\in\{1,2,3\}$.[23] The strain tensor can be quite complex, with both shear strains ($\epsilon_{ij}\neq0$ for $i\neq j$) and pure strains (only $\epsilon_{ii}\neq0$). In the literature,[24] it is customary to use the more convenient matrix notation (also called *Voigt* notation) $\epsilon_1=\epsilon_{11}$, $\epsilon_2=\epsilon_{22}$, $\epsilon_3=\epsilon_{33}$, $\epsilon_4=2\epsilon_{23}=2\epsilon_{32}$, $\epsilon_5=2\epsilon_{31}=2\epsilon_{13}$, $\epsilon_6=2\epsilon_{12}=2\epsilon_{21}$, and we will adopt this convention from here on.

Strain affects the magnetic properties of a ferromagnet because of the magnetoelastic effect.[21,24–26] As discussed in detail, e.g., by Chikazumi,[26] this effect can be quantitatively described by the magnetoelastic contribution

$$F_{magel}=B_1[\epsilon_1(\alpha_1^2-1/3)+\epsilon_2(\alpha_2^2-1/3)+\epsilon_3(\alpha_3^2-1/3)]+(1/2)B_2(\epsilon_4\alpha_2\alpha_3+\epsilon_5\alpha_3\alpha_1+\epsilon_6\alpha_1\alpha_2) \quad (1)$$

to the magnetic free energy density F, with the magnetoelastic coupling coefficients B_1 and B_2, and the direction cosines α_i between the direction of magnetization and the cubic axes.

For the scope of this paper, it is sufficient to limit the discussion of the magnetoelastic free energy term, Eq. (1), to the simple case of vanishing shear strains. This situation is encountered, for example, if stress is applied to a cubic crystal along a crystal axis (i.e., strain axis $\|$ [010], see Fig. 1), as in the experiments described in Sec. III. In this case, the resulting distortion is fully described by strain tensor components $\epsilon_i\neq0$ for $i\in\{1,2,3\}$, while $\epsilon_i=0$ for $i\in\{4,5,6\}$. As evident from Eq. (1), pure strain yields magnetic anisotropy contributions which are formally identical to first-order uniaxial anisotropy terms $F_{uniax,i}=(2K_{u,i}/M)\alpha_i^2$ along the crystalline axes.[26] Given that $B_1>0$, tensile strain along the y axis ($\epsilon_2>0$) will thus increase the free energy along this direction and therefore make it magnetically harder, while compressive strain ($\epsilon_2<0$) will make this direction easier. We note that for $B_1<0$, the situation is inverted, and that the argument can be applied analogously for strain along the x or the z axis. Both pseudomorphic growth and the piezoelectric actuator introduce strains in epitaxial ferromagnetic films and thus uniaxial magnetoelastic anisotropies along the [100], [010], and [001] directions. Epitaxial strain due to lattice mismatch usually leads to isotropic strain in the film plane. In contrast, a voltage applied to the actuator leads to tunable uniaxial anisotropies differing in both sign and magnitude. Piezoinduced strains thus allow to alter the magnetic anisotropy—and therefore to control the magnetization orientation in a ferromagnet *in situ*.

The effect of the magnetoelastic anisotropy ("stress anisotropy"), Eq. (1), on the magnetization orientation obviously depends on the magnitude of F_{magel} as compared to the magnitude of the other anisotropy contributions in a given ferromagnet. In crystalline magnets, these anisotropies are typically large, so that the magnetoelastic contribution can only modify the free energy landscape to some extent but will typically not result in qualitative changes. This situation is illustrated in Fig. 1, using $F_{magel}=K_{magel}\alpha_2^2$ and an intrinsic cubic anisotropy $F_{cubic}=K_{c1}(\alpha_1^2\alpha_2^2+\alpha_2^2\alpha_3^2+\alpha_3^2\alpha_1^2)$ with $K_{magel}/K_{c1}=-1/5$ (red curve). The straininduced uniaxial anisotropy along [010] does not qualitatively change the dominant cubic (biaxial) magnetic symmetry but rotates the two easy axes slightly towards one another. We note that if F_{magel} dominates magnetic anisotropy, a tunable magnetoelastic contribution will allow to qualitatively change the magnetic anisotropy. This situation could be realized by applying stress within the plane of, e.g., amorphous ferromagnetic films, which have negligible crystalline anisotropy.

III. EXPERIMENTAL DETAILS

The Fe_3O_4 thin films studied here were deposited on (100)-oriented MgO substrates by laser molecular beam epitaxy, as described in detail elsewhere.[27,28] For the samples discussed here, we used KrF laser pulses with a fluence of 2.5 J/cm^2 and a repetition rate of 2 Hz to ablate material from a stoichiometric Fe_3O_4 target. The growth took place in Ar atmosphere at a pressure of 0.06 mbar and at a substrate temperature of 320 °C. The structural and magnetic properties of the samples were determined via high-resolution x-ray diffraction in a Bruker AXS D8 Discover diffractometer and superconducting quantum interference device (SQUID) magnetometry in a Quantum Design MPMS XL-7, respectively. We used ferromagnetic resonance (FMR) spectroscopy in the X band (microwave frequency of ≈9.3 GHz) to quantitatively determine the magnetic anisotropy. To this end, the

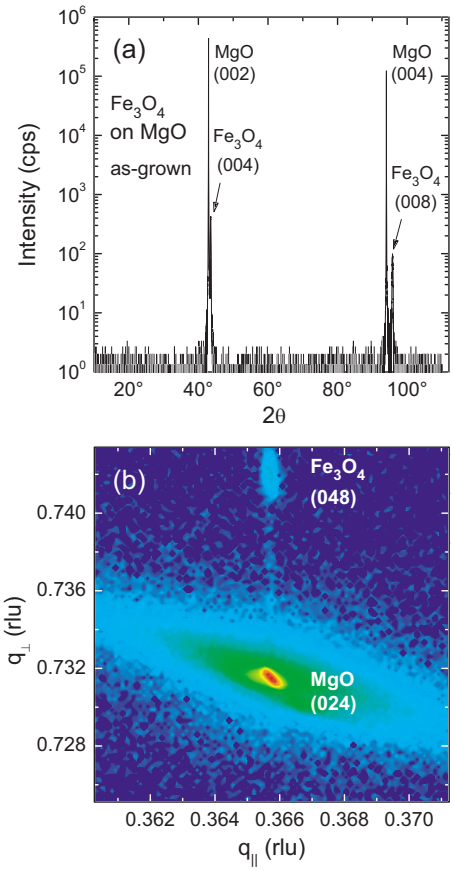

FIG. 2. (Color online) (a) 2θ-θ scan of the as-grown Fe_3O_4/MgO(001) sample. The Fe_3O_4 (004) and (008) reflections indicated by the arrows are at slightly higher angle 2θ than the (002) and (004) reflections of the MgO substrate. (b) Reciprocal space map of the Fe_3O_4 (048) and MgO (024) reflections. The Fe_3O_4 and the MgO reflections occur at the same in-plane $q_{||}$, showing that the magnetite film is coherently strained.

samples were inserted in the TE_{102} cavity of a Bruker ESP 300 spectrometer, and the FMR was recorded at room temperature using magnetic field modulation at 100 kHz with an amplitude $\mu_0 H_{mod}$=3.2 mT to allow for phase-sensitive detection.

IV. RESULTS AND DISCUSSION

We have investigated several Fe_3O_4/piezoactuator samples and obtained very reproducible results. Therefore, we here focus on a 44 nm thick Fe_3O_4 layer on MgO, which was most extensively characterized. Conventional 2θ-θ x-ray diffraction scans [Fig. 2(a)], together with reciprocal space maps [Fig. 2(b)], yield an out-of-plane Fe_3O_4 lattice constant of 0.8305 nm and an in-plane lattice constant of 0.8425 nm. The latter corresponds to twice the lattice constant of the MgO substrate within experimental error. The magnetite film is thus coherently strained, as directly evident from the reciprocal space map around the Fe_3O_4 (048) and MgO (024) reflections displayed in Fig. 2(b). The mosaic spread is very small, with a full width at half maximum $\Delta\omega$=0.04° of the rocking curve of the Fe_3O_4 (004) reflection. The magnetization measurements yield a saturation magnetization M_s =305 kA/m, which is considerably smaller than the saturation magnetization of nearly 500 kA/m of bulk magnetite.[16] Such a reduced saturation magnetization is often observed in thin Fe_3O_4 films.[29,30] It is attributed either to deviations from bulk stoichiometry[31,32] or to the presence of structural defects, in particular, antiphase boundaries.[33–35]

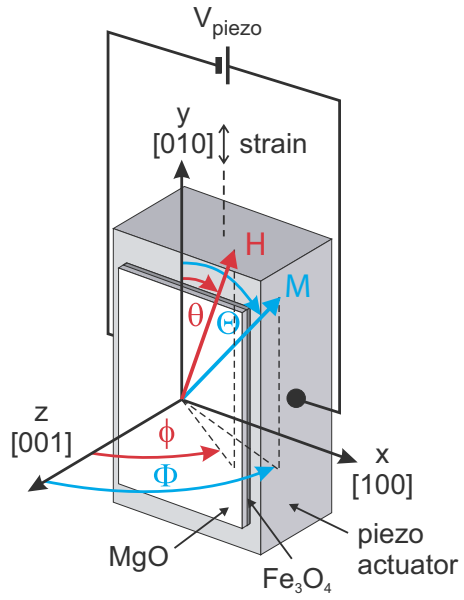

FIG. 3. (Color online) Sketch of the Fe_3O_4 film-piezoactuator sandwich and of the coordinate system used.

To allow for an *in situ* variation of the strain, we cut the sample into pieces with lateral dimensions of 2×2 mm^2 and polished the MgO substrate down to a thickness of only 50 μm. The samples are then cemented onto piezoelectric lead zirconate titanate (PZT) stack actuators[36] using a two-component epoxy.[37] The sample discussed here was cemented with the magnetite film facing the piezoelectric actuator (piezoactuator-epoxy-Fe_3O_4/MgO). In all samples, we aligned the Fe_3O_4 film in such a way that the dominant uniaxial deformation of the piezoactuator is parallel to the Fe_3O_4 [010] direction (see Fig. 3) and cured the epoxy for 1 h at 100 °C in air.

To quantify the amount of strain induced in the sample by the piezoelectric actuator, we also relied on x-ray diffraction. A direct measurement of the in-plane lattice constants and thus the strains ϵ_1 and ϵ_2 via reciprocal space maps did not prove useful for a quantitative analysis due to the wide spatial expansion of the reflections. As 2θ-θ scans allow for a determination of the out-of-plane lattice constant (and thus small strains) with much higher precision, we deduce ϵ_1 and ϵ_2 from measured ϵ_3 via elasticity theory. Since the intensity of the Fe_3O_4 reflections is too low to allow for a measurement of the Fe_3O_4 film lattice constants with sufficient accuracy, we investigated the much stronger MgO reflections in 2θ-θ scans. As evident from Fig. 4(a), the MgO reflections clearly shift with V_{piezo}. To minimize systematic errors, we used the Nelson-Riley formalism to determine the out-of-plane lattice constant c^{MgO} from these measurements.[38] The MgO lattice constant thus determined changes linearly with

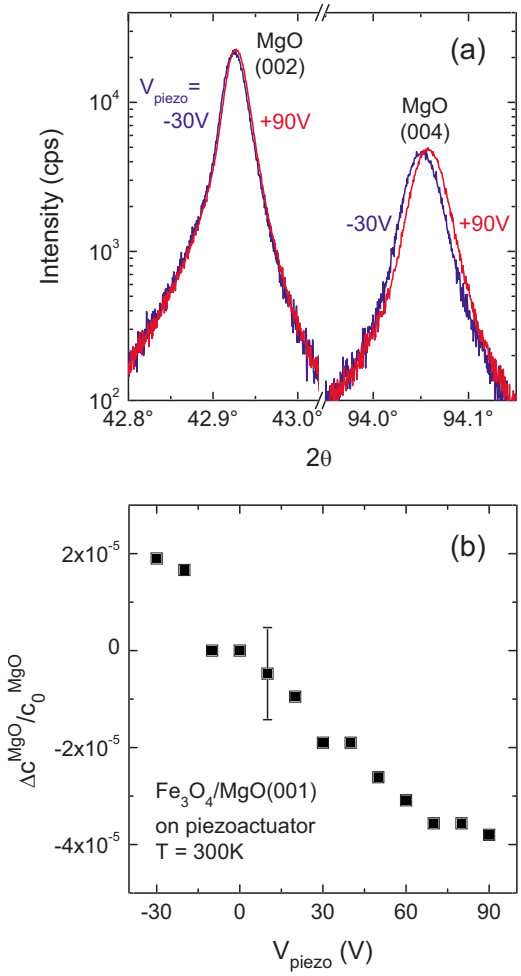

FIG. 4. (Color online) (a) The application of a finite voltage V_{piezo} to the piezoelectric actuator allows to stress the sample *in situ*. The piezoinduced stress manifests itself as a change in the sample's lattice constants, as directly evident from the 2θ-θ scans at $V_{\text{piezo}}=-30$ V and $V_{\text{piezo}}=+90$ V. (b) The out-of-plane MgO lattice constant c^{MgO} changes linearly with the voltage V_{piezo} applied to the actuator. The relative lattice constant change $\Delta c^{\text{MgO}}/c_0^{\text{MgO}}=(c^{\text{MgO}}-c_0^{\text{MgO}})/c_0^{\text{MgO}}$ is equivalent to the out-of-plane strain ϵ_3^{MgO}. The error bar corresponds to an upper estimate of the error in the determination of the lattice constants following the Nelson-Riley formalism, considering the uncertainties in the determination of the individual (002) and (004) reflections.

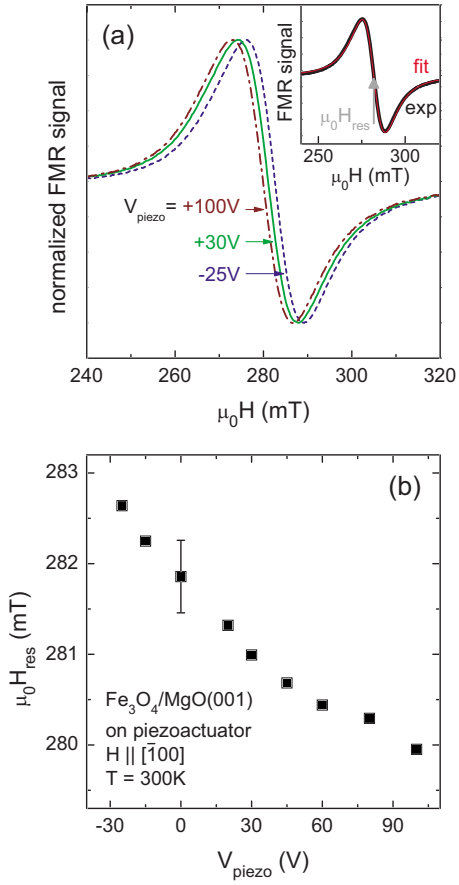

FIG. 5. (Color online) (a) Room-temperature FMR spectra of a Fe_3O_4 film mounted on a piezoelectric actuator for $\mathbf{H}\|[\bar{1}00]$ for three different bias voltages V_{piezo} applied to the actuator. The FMR spectra systematically shift with V_{piezo}. The inset shows that the FMR spectrum can be fitted with the derivative of a Lorentz curve. (b) The FMR resonance field $\mu_0 H_{\text{res}}$ changes linearly with V_{piezo} in good approximation. The error bar corresponds to the total change in the FMR peak-to-peak linewidth with V_{piezo} as an upper estimate of the uncertainty in the determination of $\mu_0 H_{\text{res}}$.

V_{piezo} [Fig. 4(b)]. We note that the relative lattice constant change $(c^{\text{MgO}}-c_0^{\text{MgO}})/c_0^{\text{MgO}}$ displayed in Fig. 4(b) equals the out-of-plane strain ϵ_3^{MgO}, where c_0^{MgO} is the lattice constant for $V_{\text{piezo}}=0$ V. As discussed in more detail in the Appendix, in the framework of elasticity theory, ϵ_3^{MgO} is sufficient to quantitatively derive the strain $\epsilon_2^{\text{MgO}}=-(c_{11}^{\text{MgO}}/c_{12}^{\text{MgO}})(1-\nu_{\text{piezo}})^{-1}\epsilon_3^{\text{MgO}}$ induced within the plane along [010]. Here, $\nu_{\text{piezo}}=0.45$ is the Poisson ratio of the piezoactuator. Using the literature values $c_{11}^{\text{MgO}}=29.66\times10^{10}$ N/m^2 and $c_{12}^{\text{MgO}}=9.59\times10^{10}$ N/m^2,[39] the overall change $\Delta\epsilon_3^{\text{MgO}}=\epsilon_3^{\text{MgO}}(+90\text{ V})-\epsilon_3^{\text{MgO}}(-30\text{ V})\approx-6\times10^{-5}$ observed experimentally corresponds to $\Delta\epsilon_2^{\text{MgO}}\approx33\times10^{-5}$. This amounts to only about 39% of the nominal stroke $\Delta\epsilon_2^{\text{piezo}}=87\times10^{-5}$ of the actuator in the voltage range $-30\text{ V}\le V_{\text{piezo}}\le+90$ V assuming a perfect linear expansion of the actuator.[40] Assuming that the 50 μm thick sample does not significantly impede the elongation of the 2 mm thick actuator, the most likely cause for the reduced $\Delta\epsilon_2^{\text{MgO}}$ value observed is the imperfect strain transmission by the cement. Careful optimization of the cementing procedure thus should allow to increase the strain introduced into the Fe_3O_4 film by up to a factor of about 2.5 in future experiments. Furthermore, a reduction of the MgO substrate thickness could have a beneficial effect on strain transmission as well.

We now turn to the ferromagnetic resonance spectra of the Fe_3O_4 film-piezoelectric actuator sandwich. Figure 5(a) shows how the room temperature FMR spectrum of the sample for $\mathbf{H}\|[\bar{1}00]$ changes as a function of the voltage V_{piezo} applied to the actuator. The FMR spectrum consists of a single resonance with a peak-to-peak linewidth of $\mu_0\delta H_{\text{p.p.}}\approx13$ mT, which is well described by a Lorentzian lineshape [inset in Fig. 5(a)]. Upon the application of $V_{\text{piezo}}>0$ V ($V_{\text{piezo}}<0$ V), which corresponds to an expansion (contraction) of the actuator along [010], as illustrated in Fig.

3, the FMR shifts to lower (higher) magnetic fields. Within the voltage range $-25\ \mathrm{V} \leq V_{\mathrm{piezo}} \leq 100\ \mathrm{V}$, in which the stroke of the actuator linearly depends on the applied voltage, the FMR resonance field $\mu_0 H_{\mathrm{res}}$ also is proportional to V_{piezo} in good approximation [Fig. 5(b)].

The shift of the FMR resonance with V_{piezo} is attributed to straininduced changes of the magnetic anisotropy of the Fe_3O_4 film. Spurious effects, such as a variation of the FMR lineshape, the microwave cavity tuning, or the temperature, can be ruled out with the following arguments. First, the peak-to-peak linewidth $\mu_0 \delta H_{\mathrm{p.p.}}$ changes by less than 0.8 mT for $-25\ \mathrm{V} \leq V_{\mathrm{piezo}} \leq 100\ \mathrm{V}$, so that a variation of the FMR *lineshape* cannot account for the maximum shift of the FMR resonance field $\mu_0 \Delta H_{\mathrm{res}} = \mu_0 H_{\mathrm{res}}(-25\ \mathrm{V}) - \mu_0 H_{\mathrm{res}}(+100\ \mathrm{V}) = 2.7$ mT observed. Second, the resonance frequency of the microwave cavity is constant to about 10^{-4} over the whole V_{piezo} range and can thus not account for the FMR line shift of $\frac{2.7\ \mathrm{mT}}{281\ \mathrm{mT}} \approx 10^{-2}$. Third, the linear dependence $H_{\mathrm{res}}(V_{\mathrm{piezo}}) \propto V_{\mathrm{piezo}}$ allows to rule out temperature fluctuations as an explanation for the effect. Most importantly, however, the evolution of $\mu_0 H_{\mathrm{res}}(V_{\mathrm{piezo}})$ with the orientation of the external magnetic field, which we discuss in detail in the next paragraph, allows to unambiguously identify strain anisotropy as the origin of the FMR line shift.

Figure 6 shows that the FMR resonance field $\mu_0 H_{\mathrm{res}}$ characteristically changes as a function of magnetic field orientation $\mathbf{H} = \mathbf{H}(\theta, \phi)$ (for definition of θ and ϕ, see Fig. 3), which allows to quantify the magnetic anisotropy in the Fe_3O_4 film. For clarity, only the data for $V_{\mathrm{piezo}} = 0$ V and the two bias voltages $V_{\mathrm{piezo}} = -30$ V and $V_{\mathrm{piezo}} = +90$ V are displayed in the figure. We note, however, that a linear dependence $H_{\mathrm{res}} \propto V_{\mathrm{piezo}}$, as shown in Fig. 5(b), is observed for other magnetic field orientations as well. Figure 6 shows that the FMR line shift $\mu_0 \Delta H_{\mathrm{res}} = \mu_0 H_{\mathrm{res}}(-30\ \mathrm{V}) - \mu_0 H_{\mathrm{res}}(+90\ \mathrm{V})$ is qualitatively different for different orientations of the external field: $\mu_0 \Delta H_{\mathrm{res}}$ is large and negative (≈ -6 mT) for $\mathbf{H} \| [010]$, vanishes for $\mathbf{H} \| [110]$, and becomes positive ($\approx +4$ mT) for $\mathbf{H} \| [100]$ [Fig. 6(a)]. Moreover, ΔH_{res} also vanishes if the field is applied perpendicular to the film plane along [001] [Fig. 6(b)]. The effect of V_{piezo} on the FMR spectrum is thus qualitatively different for $\mathbf{H}$ applied along the three cubic axes of the Fe_3O_4 film. Note also that for $\mathbf{H}$ in the film plane, the FMR dominantly exhibits a fourfold symmetry as expected for a cubic material, although the resonance fields do not coincide every 90°.

To model the angular dependence of the FMR fields for $V_{\mathrm{piezo}} = 0$ V (shown as full black circles in Fig. 6), we use the free energy density[41]

$$F = -\mu_0 MH(\sin\Theta \sin\Phi \sin\theta \sin\phi + \cos\Theta \cos\theta + \sin\Theta \cos\Phi \sin\theta \cos\phi) + K_{\mathrm{u,eff}}^{[001]} \sin^2\Theta \cos^2\Phi + K_{\mathrm{u}}^{[010]} \cos^2\Theta + \frac{1}{4} K_{\mathrm{c1}} [\sin^2(2\Theta) + \sin^4\Theta \sin^2(2\Phi)]. \quad (2)$$

The first term is the Zeeman energy. The angles Θ and Φ are polar coordinates for the magnetization vector $\mathbf{M} = \mathbf{M}(\Theta, \Phi)$ (see Fig. 3) and we assume here that the applied external field suffices to saturate the magnetization to $M_s = 305$ kA/m measured with SQUID magnetometry. The effective uniaxial anisotropy contribution $K_{\mathrm{u,eff}}^{[001]} = \frac{1}{2}\mu_0 M^2 + K_{\mathrm{u}}^{[001]}$ along [001] comprises the demagnetization contribution $\frac{1}{2}\mu_0 M^2$ and the uniaxial contribution $K_{\mathrm{u}}^{[001]} < 0$ resulting from the pseudomorphic growth of the Fe_3O_4 film, which leads to isotropic tensile strain within the film plane. These two terms cannot be separated with FMR as they have the same symmetry, but in magnetite, the main contribution to $K_{\mathrm{u,eff}}^{[001]}$ usually arises from shape anisotropy $\frac{1}{2}\mu_0 M^2 > 0$ establishing a magnetic hard axis perpendicular to the film plane in the [001] direction. $K_{\mathrm{u}}^{[010]}$ represents a uniaxial anisotropy within the film plane along [010]. This term is due to the anisotropic thermal expansion of the PZT piezoactuator. The Fe_3O_4 sample is clamped onto the actuator lattice as the two-component epoxy is cured at $T = 100$ °C. Upon cooling to room temperature, the anisotropic contraction of the actuator builds up tensile strain along the [010] direction in the plane

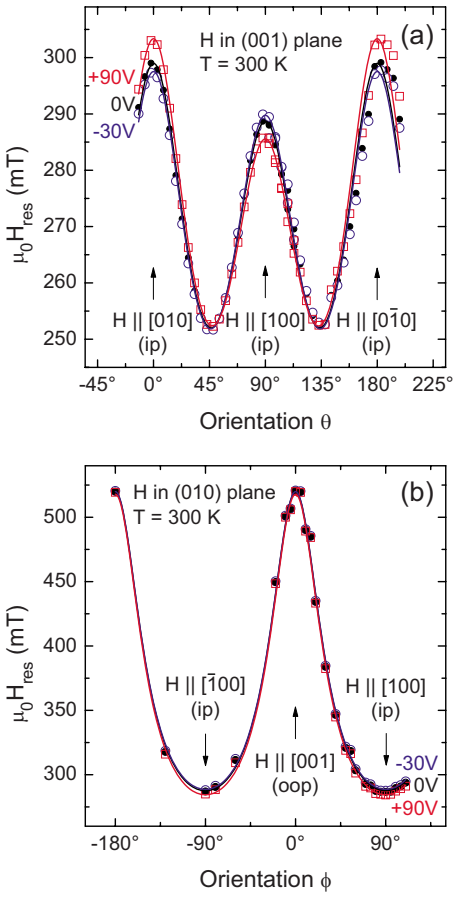

FIG. 6. (Color online) [(a) and (b)] The FMR resonance field $\mu_0 H_{\mathrm{res}}$ sensitively depends on the orientation of the external magnetic field $\mathbf{H}$ and the voltage applied to the piezoelectric actuator V_{piezo} (open circles for $V_{\mathrm{piezo}} = -30$ V, full circles for $V_{\mathrm{piezo}} = 0$ V, and open squares for $V_{\mathrm{piezo}} = +90$ V). The full lines represent the numerically simulated FMR fields (blue line for $V_{\mathrm{piezo}} = -30$ V, black line for $V_{\mathrm{piezo}} = 0$ V, and red line for $V_{\mathrm{piezo}} = +90$ V), as described in more detail in the text. For $\mathbf{H} \| [100]$ and $\mathbf{H} \| [010]$, the magnetic field is aligned in the plane of the film (ip), while it points out of plane (oop) for $\mathbf{H} \| [001]$.

of the Fe_3O_4 layer, which results in a uniaxial magnetic anisotropy. Finally, K_{c1} is the first-order cubic anisotropy constant.

The FMR resonance fields are obtained numerically from Eq. (2) by evaluating the equation of motion $(\omega/\gamma)^2 = (M^2 \sin^2\Theta)^{-1} [(\partial_\Phi^2 F)(\partial_\Theta^2 F) - (\partial_\Phi \partial_\Theta F)^2]$ at the equilibrium orientation (Θ_0, Φ_0) of the saturation magnetization given by $\partial_\Theta F|_{\Theta=\Theta_0} = \partial_\Phi F|_{\Phi=\Phi_0} = 0$.[41] The resonance fields calculated in this way using the anisotropy fields $2K_{u,eff}^{[001]}/M_s = 160.4$ mT, $2K_u^{[010]}/M_s = 6.4$ mT, and $2K_{c1}/M_s = -29.8$ mT, and $g = 2.02$, are shown as full black lines in Fig. 6. The good agreement between the simulated and the measured resonance fields for $V_{piezo} = 0$ V demonstrates that the magnetic anisotropy contributions included in Eq. (2) are sufficient to model the magnetic anisotropy of the Fe_3O_4 film within the accuracy of the experiment. The magnetic anisotropy constants for $V_{piezo} = 0$ V agree well with the values quoted in the literature[42–45]—with the exception of the uniaxial anisotropy contribution $K_u^{[010]}$ within the film plane, which is not observed in as-grown Fe_3O_4 films as the thermal expansion typically is isotropic.[42] This was verified by angular-dependent FMR measurements of the sample in the as-grown state, where $2K_{u,eff}^{[001]}/M_s = 146.3$ mT, $2K_u^{[010]}/M_s = 0$ mT, and $2K_{c1}/M_s = -29.3$ mT were found.

To describe the influence of the voltage-tunable strain induced by the piezoelectric actuator, we add the magnetoelastic contribution,

$$F_{magel} = \chi \frac{3}{2} \lambda_{100}^{Fe_3O_4} (c_{12}^{Fe_3O_4} - c_{11}^{Fe_3O_4}) \left(\frac{c_{11}^{MgO}}{c_{12}^{MgO}} \frac{1}{1-\nu_{piezo}} \right) \times \left[\nu_{piezo} (\sin^2\Theta \sin^2\Phi - 1/3) - (\cos^2\Theta - 1/3) + (1-\nu_{piezo}) \frac{c_{12}^{Fe_3O_4}}{c_{11}^{Fe_3O_4}} (\sin^2\Theta \cos^2\Phi - 1/3) \right] \epsilon_3^{MgO}, \quad (3)$$

derived in the Appendix [Eq. (A7)] to the free energy density, Eq. (2). $\lambda_{100}^{Fe_3O_4} = -19.5 \times 10^{-6}$ (Ref. 20) denotes the magnetostriction constant of bulk magnetite, $c_{11}^{Fe_3O_4} = 27.2 \times 10^{10}$ N/m^2 and $c_{12}^{Fe_3O_4} = 17.8 \times 10^{10}$ N/m^2 (Ref. 46) are the elastic moduli of bulk Fe_3O_4. The factor χ is introduced in Eq. (3) as a proportionality factor since the calculated resonance fields depend very sensitively on the elastic moduli.[46,47] χ accounts for the fact that the magnetoelastic properties of ferromagnetic thin films typically deviate from the corresponding bulk values.[48–50] Using the measured out-of-plane strain $\epsilon_3^{MgO} = \Delta c^{MgO}/c_0^{MgO}$ [Fig. 4(b)], the angular dependence of the FMR resonance fields for finite V_{piezo} can be calculated. Using $\chi = 0.7$, we obtain excellent agreement with experiment, as evident from the red and blue full lines in Fig. 6 calculated with the above values for $V_{piezo} = -30$ V and +90 V, respectively.

The piezoinduced changes in the magnetic anisotropy have a substantial impact on the free energy and the magnetization orientation. The equilibrium magnetization orientation (Θ_0, Φ_0) is given by the minima in the free energy $\partial_\Theta F|_{\Theta=\Theta_0} = \partial_\Phi F|_{\Phi=\Phi_0} = 0$ with $\partial_\Theta^2 F|_{\Theta=\Theta_0}, \partial_\Phi^2 F|_{\Phi=\Phi_0} > 0$. Using the experimentally determined anisotropy constants given above, we find that the magnetization vector is in the film plane (close to $\langle 110 \rangle$) for vanishing external magnetic field $\mu_0 H = 0$ mT. However, Θ_0 characteristically changes for finite V_{piezo}, as evident from the free energy curves shown in Figs. 7(a) and 7(b). This calculation shows that the orientation of the easy axes and thus the equilibrium magnetization orientation Θ_0 can be continuously and reversibly shifted by about 6° for $-30\ \text{V} \leq V_{piezo} \leq +90$ V in the present sample. Assuming perfect strain transmission from the piezoactuator into the sample ($\epsilon_1^{MgO} = \epsilon_1^{piezo}$ and $\epsilon_2^{MgO} = \epsilon_2^{piezo}$), the equilibrium magnetization orientation can be shifted by 17° [Fig. 7(c)]. These results show that a fully reversible, continuous, voltage-tunable control of the magnetization orientation is possible in crystalline ferromagnets attached to mechanical stressors (piezoactuators). This "piezocontrol of magnetization" does not require the application of variable magnetic fields. However, we note that care must be taken to ensure that a well defined global free energy minimum is always present to preserve a homogeneous magnetization and prevent the formation of a multidomain state.

Because the piezoelectric actuator is cemented onto the ferromagnetic crystal, it is possible to align the direction of the controllable, external stress along any direction within the ferromagnetic film plane. This allows us to engineer the type of strain exerted in the sample. For example, if the piezoactuator elongation axis is aligned along a $\langle 100 \rangle$ axis in a cubic crystal (Fig. 1), shear strain contributions are suppressed. This was the case in all the experiments discussed above. In contrast, shear strain effects will play an important role, e.g., if the piezoactuator elongation is along a $\langle 110 \rangle$ axis. The alignment degree of freedom thus opens an experimental pathway for the distinction, comparison, and selective investigation of different magnetoelastic contributions to the free energy. Furthermore, the application of ac voltages to the piezoelectric actuator will allow to periodically modulate the magnetic anisotropy with time and therefore to modulate the magnetization orientation with time. This is an interesting starting point for future experiments, e.g., for the realization of voltage-controlled, time-varying magnetic fields.

V. CONCLUSIONS AND OUTLOOK

In summary, we have investigated the interplay between strain and the magnetic anisotropy properties of a thin crystalline Fe_3O_4 film. We modified the strain in the magnetite film *in situ* by means of a piezoelectric actuator and determined the resulting modification in the lattice constants and the magnetic anisotropy via x-ray diffraction and ferromagnetic resonance experiments, respectively. We find that the strain induced by the piezoelectric actuator significantly alters the magnetic anisotropy in Fe_3O_4 at room temperature, and that these modifications can be quantitatively modeled using magnetoelastic theory. In the present sample, the piezoinduced manipulation of magnetic anisotropy allows a shift of the equilibrium magnetization orientation by 6°. Our results suggest that a perfect strain transmission across the actuator-sample interface should allow to realize magnetization orientation shifts of 17°. The possibility to exert strain

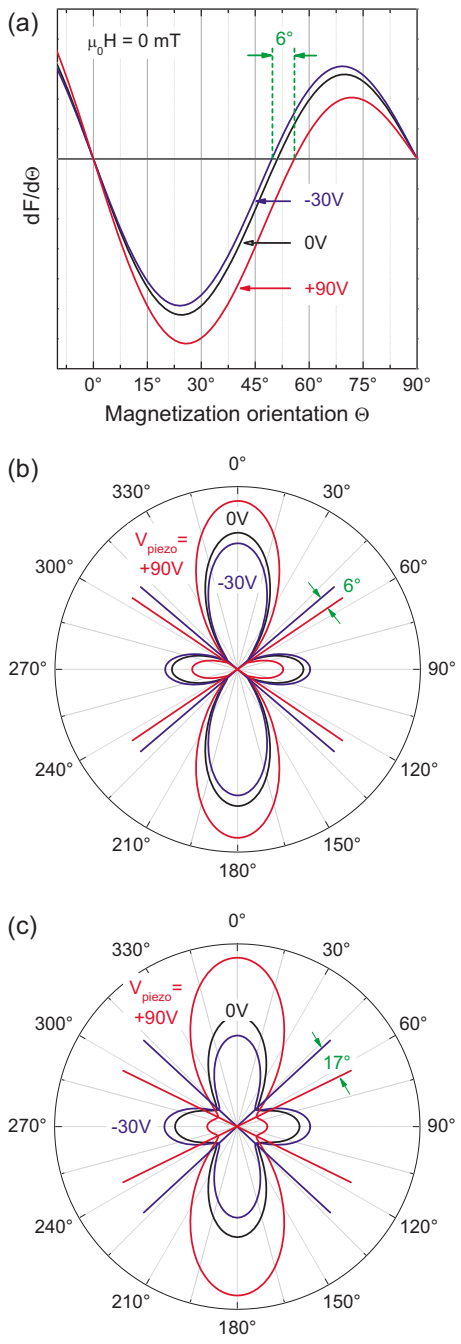

FIG. 7. (Color online) Numerical simulations of the dependence of the free energy on the magnetization orientation within the film plane for no external magnetic field applied. Panels (a) and (b) show the derivative of the free energy and the free energy, respectively, using the anisotropy parameters determined from FMR. In panel (c), we assumed a perfect strain transmission from piezoactuator to sample and no strain relaxation within the sample ($\epsilon_1^{\mathrm{MgO}}=\epsilon_1^{\mathrm{piezo}}$, $\epsilon_2^{\mathrm{MgO}}=\epsilon_2^{\mathrm{piezo}}$), which results in much larger changes in the magnetic anisotropy. The orientation of the easy magnetic axes [shown as full lines in panels (b) and (c)] clearly depends on the stress exerted by the piezoelectric actuator.

along arbitrary directions within the thin film by simply adjusting the piezoactuator elongation direction during the fabrication process of the ferromagnet-piezoactuator stack allows to investigate the different contributions to the magnetoelastic energy, in particular, the values of the magnetostriction constants λ along different crystal orientations. Furthermore, the application of ac voltages to the actuator will allow to modulate the magnetization orientation with time.

ACKNOWLEDGMENTS

The work at the Walter Schottky Institut was supported by the Deutsche Forschungsgemeinschaft (DFG) via SFB 631. The work at the Walther-Meissner-Institut was supported by the DFG via SPP 1157 (Project No. GR 1132/13) and the German Excellence Initiative via the "Nanosystems Initiative Munich (NIM)".

APPENDIX: MAGNETOELASTIC CONTRIBUTION TO FREE ENERGY

In the following, we derive the magnetoelastic contribution F_{magel} to the free energy density of a cubic crystal. F_{magel} shall be caused by the application of lateral strain *within* the plane of a thin ferromagnetic Fe_3O_4 film along a ⟨100⟩ direction. The aim hereby is to express F_{magel} only in terms of the strain component ϵ_3 *perpendicular* to the film plane, as the latter can be quantitatively measured via x-ray diffraction. Because of the elastic properties of the crystal, ϵ_3 is directly connected to the in-plane strains ϵ_1 and ϵ_2. The expression for F_{magel} sought thus links the in-plane strain anisotropy to the out-of-plane lattice parameter change.

We start from the general expression[26]

$$F_{\mathrm{magel}} = B_1[\epsilon_1(\alpha_1^2 - 1/3) + \epsilon_2(\alpha_2^2 - 1/3) + \epsilon_3(\alpha_3^2 - 1/3)] + (1/2)B_2(\epsilon_6\alpha_1\alpha_2 + \epsilon_4\alpha_2\alpha_3 + \epsilon_5\alpha_3\alpha_1), \quad \text{(A1)}$$

where α_i denote the direction cosines of the magnetization with respect to the cubic axes, B_i are the magnetoelastic coupling constants, and the strains ϵ_i are expressed in matrix notation.[23] The application of stress will deform the crystal until the magnetoelastic energy is balanced by the elastic energy of a cubic crystal[24,26]

$$F_{\mathrm{el}} = (1/2)c_{11}(\epsilon_1^2 + \epsilon_2^2 + \epsilon_3^2) + (1/2)c_{44}(\epsilon_4^2 + \epsilon_5^2 + \epsilon_6^2) + c_{12}(\epsilon_2\epsilon_3 + \epsilon_3\epsilon_1 + \epsilon_1\epsilon_2), \quad \text{(A2)}$$

with the elastic moduli c_{ij}.

Since we elongate the ferromagnetic crystal along a cubic axis in the experiments, we now restrict the discussion to pure strains and assume vanishing shear strains ($\epsilon_4=\epsilon_5=\epsilon_6=0$). To determine the strains $\epsilon_i^{\mathrm{Fe_3O_4}}$ in the ferromagnetic film, we use the fact that no stress is applied perpendicular to the film plane, i.e., $\sigma_3=\partial F_{\mathrm{el}}/\partial\epsilon_3=0$.[24] Thus, Eq. (A2) yields

$$\epsilon_3 = -\frac{c_{12}}{c_{11}}(\epsilon_1 + \epsilon_2). \quad \text{(A3)}$$

The in-plane strains ϵ_1 and ϵ_2 are related via the Poisson ratio ν according to

$$\epsilon_1 = -\nu\epsilon_2. \quad \text{(A4)}$$

We here use the Poisson ratio of the piezoelectric actuator $\nu=\nu^{\mathrm{piezo}}$, assuming that the cement transmits the strains of

the actuator into the sample in such a way that the Poisson ratio of the strained sample coincides with the one of the actuator. This is reasonable, as in the experiments, the sample is only about 50 μm thick and thus orders of magnitude thinner than the 2 mm thick piezoelectric actuator. $\nu^{\text{piezo}}=0.45$ is determined by the piezoelectric constants of the actuator, $d_{31,\text{piezo}}=-290$ pm/V and $d_{33,\text{piezo}}=+640$ pm/V.[40] As the Fe_3O_4 film is coherently strained, $\epsilon_1^{Fe_3O_4}=\epsilon_1^{MgO}$ and $\epsilon_2^{Fe_3O_4}=\epsilon_2^{MgO}$, so that $\epsilon_3^{Fe_3O_4}$ can be calculated with Eq. (A3) to

$$\epsilon_3^{Fe_3O_4}=-\frac{c_{12}^{Fe_3O_4}}{c_{11}^{Fe_3O_4}}(\epsilon_1^{Fe_3O_4}+\epsilon_2^{Fe_3O_4})=\frac{c_{12}^{Fe_3O_4}}{c_{11}^{Fe_3O_4}}\frac{c_{11}^{MgO}}{c_{12}^{MgO}}\epsilon_3^{MgO}. \tag{A5}$$

Finally, the magnetoelastic coupling constant B_1 and the magnetostriction constant λ_{100} are linked by[26]

$$\lambda_{100}=\frac{2}{3}\frac{B_1}{c_{12}-c_{11}}, \tag{A6}$$

so that Eq. (A1) can be written as

$$F_{\text{magel}}=\frac{3}{2}\lambda_{100}^{Fe_3O_4}(c_{12}^{Fe_3O_4}-c_{11}^{Fe_3O_4})\left(\frac{c_{11}^{MgO}}{c_{12}^{MgO}}\frac{1}{1-\nu}\right)\Bigg[\nu(\alpha_1^2-1/3)-(\alpha_2^2-1/3)+(1-\nu)\frac{c_{12}^{Fe_3O_4}}{c_{11}^{Fe_3O_4}}(\alpha_3^2-1/3)\Bigg]\epsilon_3^{MgO}. \tag{A7}$$

*andreas.brandlmaier@wmi.badw.de
†goennenwein@wmi.badw.de

[1] M. Ziese, Philos. Trans. R. Soc. London, Ser. A **358**, 137 (2000).
[2] A. Fert and P. Bruno, *Ultrathin Magnetic Structures* (Springer, New York, 2005), Vol. 2.
[3] W. Eerenstein, N. D. Mathur, and J. F. Scott, Nature (London) **442**, 759 (2006).
[4] M. Fiebig, J. Phys. D **38**, R123 (2005).
[5] N. A. Spaldin and M. Fiebig, Science **309**, 391 (2005).
[6] T. Lottermoser, T. Lonkai, U. Amann, D. Hohlwein, J. Ihringer, and M. Fiebig, Nature (London) **430**, 541 (2004).
[7] W. Eerenstein, M. Wiora, J. L. Prieto, J. F. Scott, and N. D. Mathur, Nat. Mater. **6**, 348 (2007).
[8] R. Ramesh and N. A. Spaldin, Nat. Mater. **6**, 21 (2007).
[9] M. Gajek, M. Bibes, S. Fusil, K. Bouzehouane, J. Fontcuberta, A. Barthélémy, and A. Fert, Nat. Mater. **6**, 296 (2007).
[10] C. Thiele, K. Dörr, O. Bilani, J. Rödel, and L. Schultz, Phys. Rev. B **75**, 054408 (2007).
[11] L. Berger, Phys. Rev. B **54**, 9353 (1996).
[12] J. C. Slonczewski, J. Magn. Magn. Mater. **159**, L1 (1996).
[13] M. Tsoi, A. G. M. Jansen, J. Bass, W.-C. Chiang, M. Seck, V. Tsoi, and P. Wyder, Phys. Rev. Lett. **80**, 4281 (1998).
[14] H. Ohno, D. Chiba, F. Matsukura, T. Omiya, E. Abe, T. Dietl, Y. Ohno, and K. Ohtani, Nature (London) **408**, 944 (2000).
[15] D. Chiba, M. Yamanouchi, F. Matsukura, and H. Ohno, Science **301**, 943 (2003).
[16] E. W. Gorter, Proc. IRE **43**, 1945 (1955).
[17] M. Fonin, Y. S. Dedkov, R. Pentcheva, U. Rüdiger, and G. Güntherodt, J. Phys.: Condens. Matter **19**, 315217 (2007).
[18] M. Shayegan, K. Karrai, Y. P. Shkolnikov, K. Vakili, E. P. D. Poortere, and S. Manus, Appl. Phys. Lett. **83**, 5235 (2003).
[19] B. Botters, F. Giesen, J. Podbielski, P. Bach, G. Schmidt, L. W. Molenkamp, and D. Grundler, Appl. Phys. Lett. **89**, 242505 (2006).
[20] L. R. Bickford, J. Pappis, and J. L. Stull, Phys. Rev. **99**, 1210 (1955).
[21] E. W. Lee, Rep. Prog. Phys. **18**, 184 (1955).
[22] G. Miao, G. Xiao, and A. Gupta, Phys. Rev. B **71**, 094418 (2005).
[23] J. F. Nye, *Physical Properties of Crystals* (Oxford University Press, New York, 1985).
[24] D. Sander, Rep. Prog. Phys. **62**, 809 (1999).
[25] C. Kittel, Rev. Mod. Phys. **21**, 541 (1949).
[26] S. Chikazumi, *Physics of Ferromagnetism*, 2nd ed. (Oxford University Press, New York, 1997).
[27] D. Reisinger, M. Schonecke, T. Brenninger, M. Opel, A. Erb, L. Alff, and R. Gross, J. Appl. Phys. **94**, 1857 (2003).
[28] J. Klein, C. Höfener, L. Alff, and R. Gross, Supercond. Sci. Technol. **12**, 1023 (1999).
[29] C.-H. Lai, P.-H. Huang, Y.-J. Wang, and R. T. Huang, J. Appl. Phys. **95**, 7222 (2004).
[30] C. A. Kleint, H. C. Semmelhack, M. Lorenz, and M. K. Krause, J. Magn. Magn. Mater. **140-144**, 725 (1995).
[31] Z. Kakol and J. M. Honig, Phys. Rev. B **40**, 9090 (1989).
[32] M. Paramês, J. Mariano, Z. Viskadourakis, N. Popovici, M. Rogalskid, J. Giapintzakis, and O. Conde, Appl. Surf. Sci. **252**, 4610 (2006).
[33] W. Eerenstein, T. Hibma, and S. Celotto, Phys. Rev. B **70**, 184404 (2004).
[34] D. T. Margulies, F. T. Parker, M. L. Rudee, F. E. Spada, J. N. Chapman, P. R. Aitchison, and A. E. Berkowitz, Phys. Rev. Lett. **79**, 5162 (1997).
[35] J.-B. Moussy *et al.*, Phys. Rev. B **70**, 174448 (2004).
[36] Part No. PSt 150/2×3/5, Piezomechanik GmbH, Germany.
[37] Part No. 45600 "UHU plus endfest 300", UHU GmbH & Co. KG, Germany.
[38] J. B. Nelson and D. P. Riley, Proc. Phys. Soc. London **57**, 160 (1945).
[39] Y. Sumino, O. L. Anderson, and I. Suzuki, Phys. Chem. Miner. **9**, 38 (1983).
[40] *Low Voltage Co-fired Multilayer Stacks, Rings and Chips for Actuation* (Piezomechanik GmbH, München, 2006).
[41] C. Bihler, M. Kraus, H. Huebl, M. S. Brandt, S. T. B. Goennenwein, M. Opel, M. A. Scarpulla, P. R. Stone, R. Farshchi, and O. D. Dubon, Phys. Rev. B **75**, 214419 (2007).
[42] S. Budak, F. Yildiz, M. Özdemir, and B. Aktas, J. Magn. Magn. Mater. **258-259**, 423 (2003).
[43] D. T. Margulies, F. T. Parker, F. E. Spada, R. S. Goldman, J. Li, R. Sinclair, and A. E. Berkowitz, Phys. Rev. B **53**, 9175 (1996).
[44] P. A. A. van der Heijden, M. G. van Opstal, C. H. W. Swüste, P. H. J. Bloemen, J. M. Gaines, and W. J. M. de Jonge, J. Magn. Magn. Mater. **182**, 71 (1998).

[45] S. Kale *et al.*, Phys. Rev. B **64**, 205413 (2001).
[46] H. Schwenk, S. Bareiter, C. Hinkel, B. Lüthi, Z. Kakol, A. Koslowski, and J. M. Honig, Eur. Phys. J. B **13**, 491 (2000).
[47] M. S. Doraiswami, Proc. Indian Acad. Sci., Sect. A **25**, 413 (1947).
[48] S. W. Sun and R. C. O'Handley, Phys. Rev. Lett. **66**, 2798 (1991).
[49] R. Koch, M. Weber, K. Thürmer, and K. H. Rieder, J. Magn. Magn. Mater. **159**, L11 (1996).
[50] D. Sander, A. Enders, and J. Kirschner, J. Magn. Magn. Mater. **200**, 439 (1999).